Proceedings of the 2000 IEEE
International Conference on Robotics & Automation
San Francisco, CA • April 2000

Reactive Mobile Manipulation using Dynamic Trajectory Tracking*

P. Ögren, M. Egerstedt, and X. Hu

{petter,magnuse,hu}@math.kth.se
Optimization and Systems Theory
Royal Institute of Technology
SE-100 44 Stockholm, Sweden

Abstract

A solution to the trajectory tracking problem for mobile manipulators is proposed that allows for the base to be influenced by a reactive, obstacle avoidance behavior. Given a trajectory for the gripper to follow, a tracking algorithm for the manipulator is designed, and at the same time the base motions are generated in such a way that the base is coordinated with the gripper. Furthermore, it is shown that the method allows arbitrary upper and lower bounds on the gripper-base distance to be set and this can be achieved without introducing deadlocks into the system. The solution also ensures that the control effort, spent on slow base motions, is kept small.

1 Introduction

In this paper, we investigate how to conduct mobile manipulation in such a way that the base motions are influenced by an appropriate, reactive obstacle avoidance behavior [2], together with an arm coordination behavior. At the same time, we want the gripper to track a reference trajectory, evolving in $\mathbb{R}^3$, in such a way that we can impose hard bounds on the gripper-base distance, which corresponds to keeping the gripper in the dextrous workspace [6], relative to the base.

This type of problem is relevant for a number of reasons. For instance, if one wants to be able to orient the gripper arbitrarily, for example when conducting fine object manipulation, then one needs to keep the gripper within this dextrous workspace. Furthermore, when lifting heavy loads, one typically do not want to extend the arm too much, because that could potentially make the platform fall over, or risk component failure due to the large required control torques. Another possible application could be mobile spray painting, where one wants to keep the gripper away from the base, in order to avoid clogging the sensors with paint.

Thus the problem that we will focus on is how to make sure that the end-effector is placed in the appropriate region, while tracking a desired trajectory in a proven stable way. This should be done at the same time as the platform is moving around in an unknown environment, which calls for a safety strategy that basically adds an obstacle avoidance behavior to the base control [1].

This paper is organized as follows: In Section 2, we design the control algorithm for the base in such a way that it is coordinated with the gripper while avoiding obstacles. We then, in Section 3, propose a dynamic, high-level gripper control, that is based on a reparameterization of the desired path, using a so called virtual vehicle approach [3], which results in stable trajectory tracking. We furthermore prove some properties about our controllers, such as stability and deadlock-avoidance in Section 4. The paper is concluded with some simulation results in Section 5.

2 Base Control

Our proposed base control is going to be composed of two reactive behaviors [1]: arm coordination and obstacle avoidance.

Before we look into them in detail, we introduce the following notation where all vectors are in an inertially fixed coordinate system (Figure 1). $\mathbf{r}_b$: vector to base. $\mathbf{r}_g$: vector to gripper. $\mathbf{r}_{dg}$: vector to desired gripper position. $\mathbf{r}_o$: vector to obstacle. $\mathbf{r}_{gb}$: vector to gripper from base. $\mathbf{r}_{ob}$: vector to obstacle from base. $\mathbf{r}_{g.err}$: vector to desired gripper position from gripper. $\mathbf{r}_{dgb}$:

*This work was sponsored in part by the Swedish Foundation for Strategic Research through its Centre for Autonomous Systems at KTH and in part by TFR.

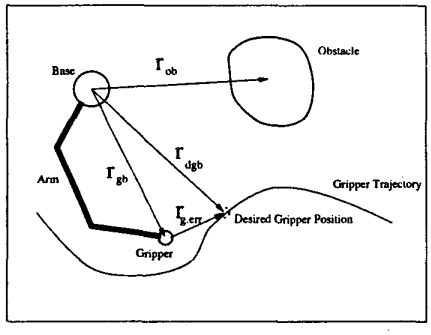

Figure 1: Notation

vector to desired gripper position from base.

2.1 The Arm Coordination Behavior

Our aim is to make the base maintain an appropriate distance to the gripper, not too far and not too close. We also introduce a dead zone that permits the faster arm to move back and forth without moving the base, as long as the arm is adequately extended.

Introduce the following parameters (all referring to the base-gripper distance):

R_{min}	–	(minimal base-gripper distance)
R_{LA}	–	(Lower Acceptable base-gripper distance)
R_{LG}	–	(Lower Good base-gripper distance)
R_{UG}	–	(Upper Good base-gripper distance)
R_{UA}	–	(Upper Acceptable base-gripper distance)
R_{max}	–	(maximal base-gripper distance)

The parameters are used in the following way. Outside of (R_{min}, R_{max}) the gripper stops and waits for the base (see gripper control). Inside of (R_{LG}, R_{UG}) the base doesn't move at all and outside of (R_{LA}, R_{UA}) it moves at full speed (in the absence of obstacles, see below and (Figure 2,3)).

Let $\hat{\mathbf{r}}_{dgb}$ be a normalized projection of $\mathbf{r}_{dgb}$ on the xy-plane.

$$\hat{\mathbf{r}}_{dgb} = \frac{(x_{dgb}, y_{dgb}, 0)}{\sqrt{x_{dgb}^2 + y_{dgb}^2}} \tag{1}$$

We then propose our arm coordination behavior as

$$\mathbf{v}_{ba} = \begin{cases} -V_{max}\hat{\mathbf{r}}_{dgb} & ||\mathbf{r}_{dgb}|| < R_{LA} \\ -V_{max}\frac{R_{LG}-||\mathbf{r}_{dgb}||}{R_{LG}-R_{LA}}\hat{\mathbf{r}}_{dgb} & R_{LA} < ||\mathbf{r}_{dgb}|| < R_{LG} \\ 0 & R_{LG} < ||\mathbf{r}_{dgb}|| < R_{UG} \\ V_{max}\left(1 - \frac{R_{UA}-||\mathbf{r}_{dgb}||}{R_{UA}-R_{UG}}\right)\hat{\mathbf{r}}_{dgb} & R_{UG} < ||\mathbf{r}_{dgb}|| < R_{UA} \\ V_{max}\hat{\mathbf{r}}_{dgb} & R_{UA} < ||\mathbf{r}_{dgb}|| \end{cases}$$

as illustrated in Figure 2.

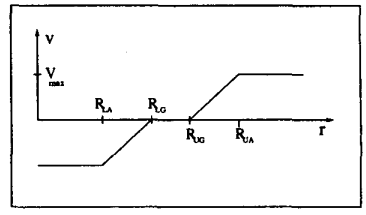

Figure 2: The control gain of the arm coordination behavior as a function of the distance between the base and the desired gripper position.

2.2 The Obstacle Avoidance Behavior

In this paper we assume that the obstacles are fairly low so they would only block the way for the base, but not that of the gripper which is mounted on the top of the base. This is reasonable since most available hardware including our Nomad XR4000 has obstacle sensors (sonars) only on the base.

In order to make the base move smoothly between the obstacles we want the obstacle avoidance behavior to be given by a repulsive vector field, generated from the sensor data.

A natural way of choosing the vector fields for small obstacles is to give them spherical symmetry. With this constructions we can also prove the absence of deadlocks (see Theorem 4.3). We let the norm of the vectors be zero outside of R_U, then increase linearly to V_{max} at R_L and be constant V_{max} inside of R_L. The direction of the vectors are radial outwards from the obstacle.

$$\mathbf{r}_{ob} = \mathbf{r}_o - \mathbf{r}_b \tag{2}$$

$$\hat{\mathbf{r}}_{ob} = \frac{\mathbf{r}_{ob}}{||\mathbf{r}_{ob}||} \tag{3}$$

$$\mathbf{v}_{bo} = \begin{cases} -V_{max}\hat{\mathbf{r}}_{ob} & ||\mathbf{r}_{ob}|| < R_L \\ -V_{max}\frac{R_U-||\mathbf{r}_{ob}||}{R_U-R_L}\hat{\mathbf{r}}_{ob} & R_L < ||\mathbf{r}_{ob}|| < R_U \\ 0 & R_U < ||\mathbf{r}_{ob}|| \end{cases}$$

This is of cause not reasonable for large objects such as walls, for them we suggest a vector field pointing outwards from the closest point on the obstacle with norm decreasing in distance as above, i.e. constant

V_{max} while inside of some R_L then decreasing to zero at some other R_U.

In order to avoid local minima we want every possible robot position to be influenced by at most one obstacle.

2.3 The Arbitration

We now apply an arbitration mechanism similar to the one suggested by Arkin [2].

$$\mathbf{v}_b = \frac{\mathbf{v}_{ba} + \mathbf{v}_{bo}}{2} \tag{4}$$

This alone gives some unstable stationary points. In order to avoid these we augment the following to our control scheme. If $\mathbf{v}_{ba} = -\mathbf{v}_{bo} \neq 0, ||\mathbf{v}_{ba}|| = V_{max}$ then we let:

$$\mathbf{v}_b = \epsilon : \epsilon \perp \mathbf{v}_{ba}, ||\epsilon|| < V_{max} \tag{5}$$

Since we have the same upper limit on both the behavior gains we have the following.

Theorem 2.1 *If* $||\mathbf{r}_{ob}|| \leq R_L$ *then* $d/dt(||\mathbf{r}_{ob}||) \geq 0$.

Proof. $||\mathbf{r}_{ob}|| \leq R_L$ which implies $||\mathbf{v}_{bo}|| = V_{max}$ and thus $d/dt(||\mathbf{r}_{ob}||) = -\mathbf{v}_b^T \mathbf{r}_{ob}/||\mathbf{r}_{ob}|| = (-\cos(\alpha)||\mathbf{v}_{ba}|| + V_{max})/2 \geq 0$ since $||\mathbf{v}_{ba}|| \leq V_{max}$. □

Thus within R_L of an obstacle the base will not move closer to it independently of the arm coordination behavior. In theorem 4.3 we show that we are still safe from deadlocks under certain assumptions.

3 The Gripper Control

Throughout the paper we make use of the fact that the arm kinematics can be decoupled from the system [5]. Let $\mathbf{r}_{dg}$ be the reference point on the trajectory that we are tracking. As in [3] we now let the motion of the point, along the trajectory, be governed by a differential equation that contains the tracking error. We furthermore augment this equation with a factor $C(\mathbf{r}_{dgb})$ that depends on the base position. This makes the combined controllers robust and it also allows us to be able to guarantee some properties that we want our system to exhibit, as will be seen in the next section.

$$\mathbf{r}_{dg} = \mathbf{r}_{dg}(s(t)) \tag{6}$$

$$\dot{\mathbf{r}}_{dg} = \mathbf{r}'_{dg}\dot{s} \tag{7}$$

$$\mathbf{r}_{g.err} = \mathbf{r}_{dg} - \mathbf{r}_g \tag{8}$$

$$\dot{s} = \frac{1}{||\mathbf{r}'_{dg}||} v_0 e^{-||\mathbf{r}_{g.err}||} C(\mathbf{r}_{dgb}) \tag{9}$$

$$\dot{\mathbf{r}}_{dg} = \mathbf{r}'_{dg} \frac{1}{||\mathbf{r}'_{dg}||} v_0 e^{-||\mathbf{r}_{g.err}||} C(\mathbf{r}_{dgb}) \tag{10}$$

The coordination factor (see Figure 3) is given by:

$$C(\mathbf{r}_{dgb}) = \begin{cases} 0 & ||\mathbf{r}_{gb}|| < R_{min} \\ \left(1 - \frac{R_{LG} - ||\mathbf{r}_{dgb}||}{R_{LG} - R_{min}}\right) & R_{min} < ||\mathbf{r}_{dgb}|| < R_{LG} \\ 1 & R_{LG} < ||\mathbf{r}_{dgb}|| < R_{UG} \\ \frac{R_{max} - ||\mathbf{r}_{dgb}||}{R_{max} - R_{UG}} & R_{UG} < ||\mathbf{r}_{dgb}|| < R_{max} \\ 0 & R_{max} < ||\mathbf{r}_{dgb}|| \end{cases} \tag{11}$$

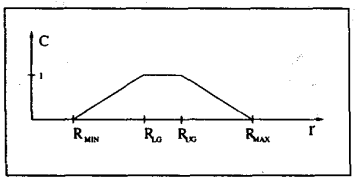

Figure 3: The coordination factor $C(\mathbf{r}_{dgb})$

Thus we stop the desired gripper position $\mathbf{r}_{dg}$ if $||\mathbf{r}_{dgb}|| \notin (R_{min}, R_{max})$. It remains still until the base has catched up i.e. $||\mathbf{r}_{dgb}|| \in (R_{min}, R_{max})$. To make the gripper track $\mathbf{r}_{dg}$ a simple proportional controller is proposed.

$$\mathbf{v}_g = \gamma \mathbf{r}_{g.err} \tag{12}$$

Where γ can be any positive constant.

4 Performance Analysis

We will show the following:

- The base will avoid obstacles and get within (R_{min}, R_{max}) of $\mathbf{r}_{dgb}$ in finite time. (Theorem 4.1 and 4.2)
- The system will not stop in a deadlock. (Theorem 4.3).
- The upper and lower bounds on the gripper-base distance can be arbitrarily set. (Theorem 4.4).
- The non-transient gripper error can be made arbitrarily small (Theorem 4.5).

These properties together show that the suggested control scheme should perform well.

The first property assures that the base moves efficiently around the obstacles. The second property shows that we are always making progress and stops in the desired gripper position are only momentary. The third property assures that the workspace of the

arm is bounded. Thus we can ensure that the gripper control does not try to move the gripper outside of its hardware limits. Or, if we want the gripper in the dextrous workspace at all times, this can also be achieved by setting the appropriate bounds. We note that not over extending the arm is also important if we are carrying a heavy load, extending the arm too far can cause tipping or other failures due to the large torques. Finally the fourth property verifies that the trajectory tracking works.

4.1 The Base-Gripper Dynamics

Since there are many trajectories that are impossible to follow we need the following definition of a feasible trajectory-obstacle combination.

Definition 4.1 *A feasible trajectory has the following properties:*

- *There exists a base trajectory in the xy-plane such that every point on the gripper trajectory is less that R_{max} away from a point on the base trajectory and every point on the base trajectory has $||\mathbf{v}_{ob}|| < V_{max}$.*
- *There is no point within R_{max} from the trajectory under influence of more than one obstacle.*
- *Every obstacle except walls has a spherical obstacle avoidance field.*

We are now ready to state our main theorem about the base control. Note that we have already shown that the base will never run into an obstacle (Theorem 2.1).

Theorem 4.1 *If the trajectory is feasible and $||\mathbf{r}_{dgb}(t)|| > R_{max}$ then there exists a finite $T > 0$, such that*

$$||\mathbf{r}_{dgb}(t+T)|| < R_{max}$$

Proof.

We first note that $||\mathbf{r}_{dgb}(t)|| > R_{max}$ means that $||\mathbf{v}_{ba}|| = V_{max}$ towards $\mathbf{r}_{dg}$ (2) and that $\dot{s} = 0$ (11). Now if we can show that $\exists \epsilon < 0 : d/dt(||\mathbf{r}_{dgb}||) \leq \epsilon \forall \mathbf{r}_{dgb} : ||\mathbf{r}_{dgb}|| > R_{max}$ we are done. We consider one obstacle with spherical repulsive field, walls can not come in between the gripper and the base.

Consider polar coordinates (r, ϕ) with the obstacle in the origin and $\mathbf{r}_{dg}$ in direction $\phi = 0$ at $r = x$ (see Figure 4).

Let the current position of the robot be (r, ϕ) with $\phi \in [0, \pi)$. If we start at $\phi = \pi$ we will get out of there instantly (5) and have a new $\phi \in [0, \pi)$.

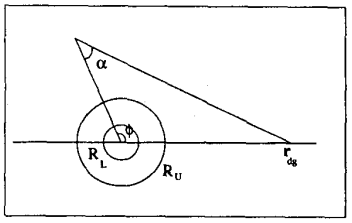

Figure 4: Polar coordinates for the proof

Some calculations give that $\dot{\phi} = -\sin(\phi)k/r$, for some $k > 0$ thus $\dot{\phi} \leq 0$.

Let α be the angle between the obstacle and the reference point (see Figure 4). The law of sines now gives: $\frac{\sin(\alpha)}{x_{obs}} = \frac{\sin(\alpha+\phi)}{r}$ which can be rewritten as:

$$\alpha(\phi, r) = -\arctan(\frac{x_{obs}\sin(\phi)}{-r + x_{obs}\cos(\phi)}). \quad (13)$$

Furthermore:

$$\cos(\alpha(\phi, r)) = \frac{\text{sgn}(r - x_{obs}\cos(\phi))}{\sqrt{1 + \frac{x_{obs}{}^2(\sin(\phi))^2}{(-r+x_{obs}\cos(\phi))^2}}}, \quad (14)$$

and we see that $\cos(\alpha(\phi, r))$ increases with r. A differentiation gives:

$$\frac{\partial}{\partial\phi}\alpha(\phi, r) = -\frac{x_{obs}\,(-\cos(\phi)r + x_{obs})}{r^2 - 2\,r x_{obs}\cos(\phi) + x^2} \quad (15)$$

and we notice that α is concave in ϕ and thus the maxima are found at the endpoints of an interval.

Now let us look at $d/dt(||\mathbf{r}_{dgb}||)$ when the reference point stands still and $||\mathbf{v}_{ba}|| = V_{max}$. In this case we have that

$$d/dt(||\mathbf{r}_{dgb}||) = -V_{max} + ||\mathbf{v}_{ob}||cos(\alpha) \quad (16)$$

Consider the three regions: $r > x + \delta$, $r < x, \phi < \arccos(r/x)$, $\phi_L \leq \phi \leq \phi_U$.

Since the trajectory is feasible we can choose $\delta > 0$ s.t. $R_L - x < \delta < R_{max}$. Now ϕ_L can be choosen small enough that these three regions cover the area traversable by a robot starting at $\phi = \phi_U$, outside of an R_{max}-ball around $(\phi = 0, r = x)$. If we can show that $d/dt(||\mathbf{r}_{dgb}||) < \epsilon < 0$ fore some ϵ in these regions we are done. For the first region:$r > x + \delta$ we notice that $||\mathbf{v}_{ob}|| < V_{max}$ and we set $\epsilon_1 = -V_{max} + ||\mathbf{v}_{ob}(x + \delta)|| < 0$ which is a upper bound on $d/dt(||\mathbf{r}_{dgb}||)$ for the region. For the second region: $r < x, \phi < arccos(r/x)$ we notice that $cos(\alpha(r, \phi) < 0$ and thus $\epsilon_2 = -V_{max}$ is an upper bound. For the third region: $\phi_L \leq \phi \leq \phi_U$ We see that $\cos(\alpha(\phi, r))$

increases with r and has maxima in the ϕ directions at the interval boundaries. Thus we set: $\epsilon_3 = -V_{max} + \max(\cos(\alpha(\phi_L, R_U)), \cos(\alpha(\phi_L, R_U)))$ as a upper bound. Now we set $\epsilon = \max(\epsilon_1, \epsilon_2, \epsilon_3)$ and our upper bound is done. We have that $d/dt(||\mathbf{r}_{dgb}||) \leq \epsilon < 0$ while $||\mathbf{r}_{dgb}|| > R_{max}$. □

Theorem 4.2 *If the trajectory is feasible and* $||\mathbf{r}_{dgb}(t)|| < R_{min}$ *then there exists a finite* $T > 0$ *such that*

$$||\mathbf{r}_{dgb}(t+T)|| > R_{min}$$

The proof is similar to that of Theorem 4.1 and more straight forward, thus it is omitted here.

Theorem 4.3 *If the trajectory is feasible there will never be a deadlock, i.e.* $\forall t_0$ *such that* $\dot{s}(t_0) = 0$ $\exists t_1 > t_0 : \dot{s}(t_1) \neq 0$.

Proof. If $\dot{s}(t_0) = 0$ then $||\mathbf{r}_{dgb}|| \notin (R_{min}, R_{max})$. Theorems 4.1 and 4.2 shows that we will be in (R_{min}, R_{max}) in finite time and thus (11) gives that $\exists t_1 > t_0 : \dot{s}(t_1) \neq 0$. □

Theorem 4.4 *The upper and lower bounds on the base-gripper distance can be set arbitrarily.*

$$R_{min} - ||\mathbf{r}_{g.err}|| \leq ||\mathbf{r}_{gb}|| \leq R_{max} + ||\mathbf{r}_{g.err}|| \quad (17)$$

Remark. Note that this bounds the real base gripper distance since $||\mathbf{r}_{g.err}||$ is bounded by Theorem 4.5. The right choice of (R_{min}, R_{max}) can thus guarantee that the gripper is always in the reachable or dextrous workspace and keeps the arm out of singularities.

Proof. We only show that the upper bounds hold. The lower bounds can be done similarly. If the distance between the desired gripper position and the base is greater than or equal to R_{max}, the desired gripper position stops (11) and $||\mathbf{v}_{ba}|| = V_{max}$ implies $d/dt(||\mathbf{r}_{dgb}||) = -\mathbf{v}_b^T \mathbf{r}_{dgb}/||\mathbf{r}_{dgb}|| = (-V_{max} - \cos(\alpha)||\mathbf{v}_{bo}||)/2 \leq 0$ since $||\mathbf{v}_{bo}|| \leq V_{max}$. Thus

$$||\mathbf{r}_{dgb}|| \leq R_{max} \quad (18)$$

And of cause: $||\mathbf{r}_{gb}|| \leq ||\mathbf{r}_{dgb}|| + ||\mathbf{r}_{g.err}||$ which implies that

$$||\mathbf{r}_{gb}|| \leq R_{max} + ||\mathbf{r}_{g.err}||. \quad (19)$$

□

4.2 The Gripper Error

Theorem 4.5 *While in the reachable workspace, the non-transient gripper error can be made arbitrarily small by adjusting* γ*:*

$$||\mathbf{r}_{g.err}|| < ||e^{-\gamma t}\mathbf{r}_{g.err}(0)|| + (1 - e^{-\gamma t})/\gamma \quad (20)$$

Proof.

$$\begin{aligned} \dot{\mathbf{r}}_{g.err} &= \dot{\mathbf{r}}_{dg} - \dot{\mathbf{r}}_g \\ &= \frac{\mathbf{r}'_{dg}}{||\mathbf{r}'_{dg}||} v_0 e^{-||\mathbf{r}_{g.err}||} C(\mathbf{r}_{dgb}) - \gamma \mathbf{r}_{g.err} \\ &= u(t) + A\mathbf{r}_{g.err} \end{aligned} \quad (21)$$

Thus we can view the evolution of $\mathbf{r}_{g.err}$ as a linear system with input. Solving the above equation, we get

$$\mathbf{r}_{g.err} = e^{-\gamma t}\mathbf{r}_{g.err}(0) + \mathbf{a}(t) \quad (22)$$

where

$$\mathbf{a}(t) = \int_0^t e^{-\gamma(t-s)} \frac{\mathbf{r}'_{dg}}{||\mathbf{r}'_{dg}||} v_0 e^{-||\mathbf{r}_{g.err}||} C(\mathbf{r}_{dgb}) ds. \quad (23)$$

Then,

$$\begin{aligned} ||\mathbf{a}(t)|| &\leq \int_0^t |e^{-\gamma(t-s)}| \cdot ||\frac{\mathbf{r}'_{dg}}{||\mathbf{r}'_{dg}||}|| \cdot 1 \cdot 1 ds \\ &= (1 - e^{-\gamma t})/\gamma. \end{aligned} \quad (24)$$

Therefore,

$$||\mathbf{r}_{g.err}|| \leq ||e^{-\gamma t}\mathbf{r}_{g.err}(0)|| + (1 - e^{-\gamma t})/\gamma \quad (25)$$

Thus the upper bound of the tracking error as time evolves can be made arbitrarily small by adjusting γ. □

5 Simulation Results

We have two plots of the same simulation. Figure 5 shows a 3d visualization of the scene with images of the robot at different times.

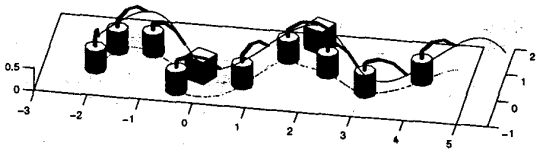

Figure 5: Simulation results, large R_{max} (3d view)

Figure 6 shows the curves from above with lines connecting the concurrent base and gripper positions. Note that the gripper curve is a sinus and the base curve is more irregular. The repulsive zones of the obstacles are dotted and one can see how the base trajectory avoids them and keeps in reach of the gripper. Far away from obstacles the base takes a shorter path than the gripper thus decreasing slow base motions.

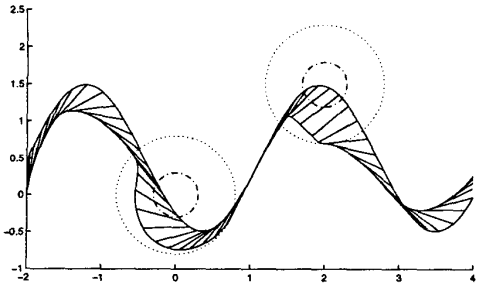

Figure 6: Simulation results (top-view), $R_{LG} = 0.3$, $R_{UG} = 0.6$, $R_{UA} = 0.8$, $R_{max} = 0.9$

In Figure 7 we see the same situation with smaller R-parameters that are close to being infeasible. Specially note the different behavior close to the second obstacle. After it there is a kink where the base stands still after backing away from the obstacle.

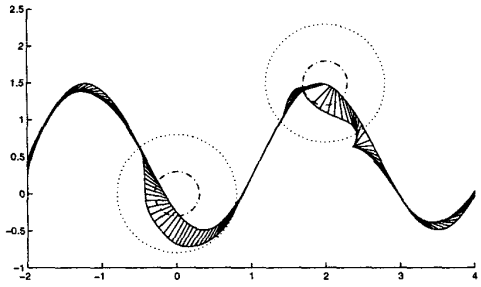

Figure 7: Simulation results (top-view), $R_{LG} = 0.25$, $R_{UG} = 0.3$, $R_{UA} = 0.35$, $R_{max} = 0.4$

In Figure 8 $||\mathbf{r}_{dgb}||$ and $\dot{s}$ can be seen. The upper figure has two peaks, one at each obstacle. We see that the gripper-base distance is larger than R_{UA} at the passing of the second obstacle and smaller than R_{LG} and thus the robot is backing right after that. In the lower figure we see that $\dot{s}$ is dominated by the $1/||\mathbf{r}'_{dg}||$ factor in (9) having a maximum at each extreme of the sinus. But notice how the third peak in $\dot{s}$ is reversed by the $C(\mathbf{r}_{dgb})$ factor at the second obstacle, thus giving more time for the base to move.

6 Conclusions

In this paper, we show how trajectory tracking with the gripper of a mobile manipulator can be performed in a systematic, and stable way, at the same time as we allow for the base to be influenced by reactive, safety behaviors. This implies that our strategy is useful, not only as a highly specialized manipulation scheme, but

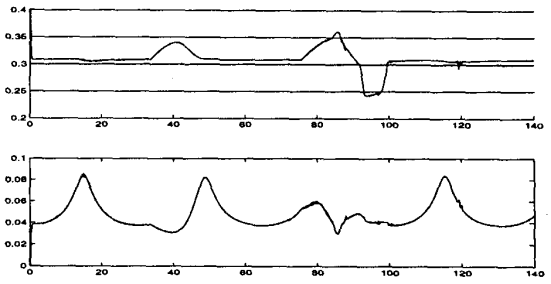

Figure 8: Simulation results, $||\mathbf{r}_{dgb}||$ (upper) and $\dot{s}$ (lower) $R_{LG} = 0.25$, $R_{UG} = 0.3$, $R_{UA} = 0.35$, $R_{max} = 0.4$

also as an integrated part in a behavior based control system for mobile, autonomous manipulators. In this paper, we furthermore prove some useful properties about our coordination strategy, and we are able to prove that, given certain assumptions on the physical features of the obstacles, the mobile manipulator stays away from dead-lock situations. We also show that the arm tracks its desired reference trajectory in a globally stable way, at the same time as the base is placed in an adequate position, from a manipulability point of view. Simulation results indicate that our control approach does not only work in theory, but also has a good chance of being useful in practice.

References

[1] R.C. Arkin and D.C. Mackenzie. Planning to Behave: A Hybrid Deliberative/Reactive Robot Control Architecture for Mobile Manipulation. *ISRAM '94*, Maui, Hawaii, 1994.

[2] R.C. Arkin. *Behavior-Based Robotics.* The MIT Press, Cambridge, Massachusetts, 1998.

[3] M. Egerstedt, X. Hu, and A. Stotsky. Control of a Car-Like Robot Using a Virtual Vehicle Approach. *37th IEEE Conference on Decision and Control*, Tampa, Florida, Dec. 1998.

[4] O. Khatib, K.Yokoi, K.Chang, D.Ruspini, R.Holmberg, A.Casal, and A.Baader. Force Strategies for Cooperative Tasks in Multiple Mobile Manipulation Systems. *International Symposium of Robotics Research*, Munich, October 1995.

[5] M. Egerstedt, and X. Hu. Coordinated Trajectory Following for Mobile Manipulation *IEEE Conference on Robotics and Automation*, San Francisco, California, April. 2000

[6] R.M. Murray, Z. Li, and S. Sastry. *A Mathematical Introduction to Robotic Manipulation.* CRC Press, 1994.